Introduction to Gaussian Beams

Prof. Elias N. Glytsis

November 4, 2021

School of Electrical & Computer Engineering
National Technical Univerity of Athens

This page was intentionally left blank.....

Contents

This page was intentionally left blank.....

1 Introduction

A ray does not provide any information about the electromagnetic field's amplitude, phase, or even spatial extent. Furthermore, plane waves are simple solutions of the Maxwell's equations but they have infinite extent and they cannot represent accurately the beam produced by a laser source. Practical laser beams are most of the time well collimated and of finite extent. Therefore, a more accurate description of optical beams and laser resonators is necessary. This can be accomplished by an approximate solution of the wave equation under what is known as the "paraxial approximation" and the corrsponding "paraxial wave equation." This approximate but analytic solution of the paraxial wave equation is known as "Gaussian Beam" [1, 2]. The Gaussian beam solutions fit well to the laser cavities and can successfully represent laser beams in most practical cases.

Most of the optical beams that propagate through free space can be characterized as TEM (i.e., they have transverse to the direction of propagation, electric and magnetic fields). From Maxwell's equations it is well known that for a source free region the Gauss law can be written in the form (for isotropic homogeneous media) [2]:

$$\vec{\nabla} \cdot \vec{D} = 0 \Longrightarrow \vec{\nabla} \cdot \vec{E} = 0, \tag{1}$$

where, $\vec{D}$ and $\vec{E}$ are the displacement vector (electric flux density) and the electric field vector, respectively. Splitting the divergence operator into a transverse and a longitudinal component (assuming that z is the propagation direction) the previous equation can be written as

$$\vec{\nabla} \cdot \vec{E} = 0 \Longrightarrow \vec{\nabla}_t \cdot \vec{E}_t + \frac{\partial E_z}{\partial z} = 0, \tag{2}$$

where $\vec{E} = \vec{E}_t + E_z \hat{z}$, with $\vec{E}_t$ and E_z the transverse and the longitudinal electric field components, respectively. Using the approach described by Verdeyen [2] and assuming that the most significant phase variation along the z direction is of the form $\exp(-jkz)$ [where the wavenumber $k = k_0 n = (\omega/c)n = (2\pi/\lambda_0)$, with n the medium refractive index, ω the radial frequency of the electromagnetic wave, λ_0 is the freespace wavelength, and c the speed of light in freespace]. At optical frequencies, the following approximations can be made:

$$\frac{\partial E_z}{\partial z} \simeq -j\frac{2\pi}{\lambda_0} n E_z, \tag{3}$$

$$\vec{\nabla}_t \cdot \vec{E}_t = \lim_{\Delta S \to 0} \left\{ \frac{1}{\Delta S} \oint_{\Delta \ell} \vec{E}_t \cdot \hat{\imath}_{\perp \ell} d\ell \right\} \simeq \lim_{D \to 0} \left\{ \frac{4}{\pi D^2} |\vec{E}_t| \pi D \right\} \simeq \frac{|\vec{E}_t|}{D}, \tag{4}$$

where D is the electromagnetic beam's finite diameter. Using the last two approximations, the relation between the longitudinal and the transverse electric field components becomes

$$|E_z| \simeq \frac{\lambda_0}{2\pi n D} |\vec{E}_t|. \tag{5}$$

The ratio $\lambda_0/(2\pi nD)$ is small ($<10^{-3}$) for visible wavelengths ($0.4\,\mu m \lesssim \lambda_0 \lesssim 0.7\,\mu m$) and beam diameters of the order of a centimeter. Therefore, the longitudinal electric field component E_z can be neglected as compared to the transverse electric field component, resulting to a TEM solution of the electromagnetic field of a Gaussian beam. Consequently, a solution for the electromagnetic beam of the form

$$\vec{E}(x,y,z) = \hat{t}E_0\psi(x,y,z)\exp(-jkz), \tag{6}$$

is sought where $\hat{t}$ is a unit vector in the transverse direction (in the xy plane) that is independent of the the x, y, z variables. Then, the electric field of Eq. (6) should satisfy the scalar Helmholtz's equation:

$$\nabla^2 E + k_0^2 n^2 E = 0. \tag{7}$$

Inserting the form of the electric field of Eq. (6) into Eq. (7) results in the following equation:

$$\nabla_t^2\psi - j2k\frac{\partial\psi}{\partial z} + \frac{\partial^2\psi}{\partial z^2} = 0, \tag{8}$$

where ∇_t is the transverse gradient operator. At this point it is assumed that the function ψ is slowly varying along the z direction since the "fast" z-variation is included in the $\exp(-jkz)$ term. If $|\partial^2\psi/\partial z^2| \ll 2k|\partial\psi/\partial z|$ (slow variation of ψ along z as compared to the wavelength) then the second derivative of ψ with respect to z in Eq. (8) can be neglected resulting in the following equation, which is known as the "paraxial wave equation,"

$$\nabla_t^2\psi - j2k\frac{\partial\psi}{\partial z} \simeq 0, \qquad \text{if} \quad \left|\frac{\partial^2\psi}{\partial z^2}\right| \ll 2k\left|\frac{\partial\psi}{\partial z}\right|. \tag{9}$$

2 Fundamental Gaussian Beam Solution

In order to find the simplest possible solution Eq. (9) is expressed in the cylindrical coordinate system assuming azimuthal independence. This means that $\psi = \psi(r_{_T}, z)$ where $r_{_T} = (x^2 + y^2)^{1/2}$ is the transverse radial distance. Then Eq. (9) can be written as

$$\frac{1}{r_{_T}}\frac{\partial}{\partial r_{_T}}\left(r_{_T}\frac{\partial\psi}{\partial r_{_T}}\right) - j2k\frac{\partial\psi}{\partial z} = 0. \tag{10}$$

Now a solution of the following form is sought:

$$\psi = \exp\left\{-j\left[P(z) + \frac{kr_{_T}^2}{2q(z)}\right]\right\}, \tag{11}$$

where $P(z)$ and $q(z)$ are unknown function that must be determined in order to satisfy Eq. (10). Substituting the last equation in Eq. (10) results in

$$\left\{ \left[\frac{k^2}{q^2(z)} \left(q'(z) - 1 \right) \right] r_{_T}^2 \;\; - \;\; 2k \left[P'(z) + \frac{j}{q(z)} \right] r_{_T}^0 \right\} \psi = 0, \qquad \forall r_{_T} \tag{12}$$

$$\frac{dq}{dz} = q'(z) \;\; = \;\; 1, \tag{13}$$

$$\frac{dP}{dz} = P'(z) \;\; = \;\; -\frac{j}{q(z)}. \tag{14}$$

It is straightforward to show that the solution of Eq. (13) is of the form $q(z) = z + jz_0$ (where z_0 is real) in order for the electromagnetic beam's intensity, $I \sim |\psi|^2$ to show $r_{_T}$-dependence in the transverse direction [2]. This can be easily realized if $|\psi(r_{_T}, z = 0)|^2 = \exp(-kr_{_T}^2/z_0)$ is considered (where imaginary value of z_0 leads to no radial dependence of $|\psi(r_{_T}, z = 0)|^2$ and it is not an acceptable solution for a beam with transverse confinement). The variable z_0 is named "Rayleigh distance" of "Rayleigh range" and can be related to what is known as "minimum spot size" or "minimum beam waist", w_0, of the Gaussian beam solution. If $|\psi(r_{_T}, z = 0)| = \exp(-r_{_T}^2/w_0^2)$ (Gaussian profile of the beam in the transverse direction) w_0 and z_0 can be related by

$$w_0^2 = \frac{2z_0}{k} = \frac{\lambda_0 z_0}{n\pi} \Longrightarrow z_0 = \frac{\pi n w_0^2}{\lambda_0}. \tag{15}$$

Using the general solution for $q(z)$ the $1/q$ factor can be written in the form:

$$\frac{1}{q(z)} \;\; = \;\; \frac{z}{z^2 + z_0^2} - j\frac{z_0}{z^2 + z_0^2} = \frac{1}{R(z)} - j\frac{\lambda_0}{\pi n w^2(z)}, \tag{16}$$

$$w^2(z) \;\; = \;\; w_0^2 \left[1 + \left(\frac{z}{z_0} \right)^2 \right], \tag{17}$$

$$R(z) \;\; = \;\; z \left[1 + \left(\frac{z_0}{z} \right)^2 \right]. \tag{18}$$

The parameter $q(z)$ is also referred as a complex radius of curvature of the Gaussian beam. Using $q(z)$ the solution for $P(z)$ can be easily from Eq. (14) as

$$jP(z) = \ln \left[1 - j \left(\frac{z}{z_0} \right) \right] = \ln \left[1 + \left(\frac{z}{z_0} \right)^2 \right]^{1/2} - j \tan^{-1} \left(\frac{z}{z_0} \right). \tag{19}$$

Applying the solutions for $q(z)$ and $P(z)$ into Eq. (11) the complete expression of the fundamental lowest-order (named as TEM_{00}) Gaussian beam is summarized as follows:

$$E_{00}(r_{_T}, z) = \mathcal{E}_0 \underbrace{\frac{w_0}{w(z)} \exp \left[-\frac{r_{_T}^2}{w^2(z)} \right]}_{\text{amplitude factor}} \underbrace{\exp \left\{ -j \left[kz - \tan^{-1} \left(\frac{z}{z_0} \right) \right] \right\}}_{\text{longitudinal phase factor}} \underbrace{\exp \left[-j \frac{kr_{_T}^2}{2R(z)} \right]}_{\text{radial phase factor}}. \tag{20}$$

A simple Gaussian beam solution is shown in Fig. 1a and sample radial profiles for various distances from its center ($z = 0$) are also shown in Fig. 1b. A snapshot in time of the Gaussian beam electric field of Eq. (20) is shown in Fig. 2a and a snapshot of its intensity $|E_{00}(r_{_T}, z)|^2$ is shown in Fig. 2b

2.1 Gaussian Beam Divergence

The Gaussian beam, like every electromagnetic wave solution, shows diffraction effects. These effects result to expansion of the beam as it propagates from the plane, $z = 0$ where it has its minimum waist size w_0. The Gaussian beam's expansion is evident from the increase of its beam waist $w(z)$ as function of z in Eq. (17). For large distances (i.e., when $z \gg z_0$) from Eq. (17) the beam waist becomes

$$w(z) \simeq \frac{w_0 z}{z_0} = \frac{\lambda_0 z}{\pi n w_0}, \tag{21}$$

and the divergence angle θ (shown in Fig. 1a) can be easily determined by

$$\tan\theta = \frac{dw(z)}{dz} = \frac{\lambda_0}{\pi n w_0} \Longrightarrow \Delta\theta = 2\theta \simeq \frac{2\lambda_0}{\pi n w_0} = \frac{4}{\pi}\,\frac{\lambda_0/n}{D_0}, \tag{22}$$

where $\Delta\theta$ is the asymptotic angular expansion of the Gaussian beam and $D_0 = 2w_0$ is its minimum diameter (defined in terms of the $1/e$ field points). In the last equation the approximation $\tan\theta \simeq \theta$ was utilized which is valid for relatively small θ's.

2.2 Gaussian Beam Power

Another important property of the Gaussian beam is that the solution described by Eq. (20) conserves power. This can be shown by determining the total power crossing any arbitrary transverse plane (for any arbitrary z distance). The total power carried by the Gaussian beam is

$$P(z) = \frac{1}{2\eta}\int_{-\infty}^{+\infty}\int_{-\infty}^{+\infty} |E_{00}|^2 dxdy = \frac{1}{2\eta}\int_{-\infty}^{+\infty}\int_{0}^{2\pi} |E_{00}(r_{_T}, z)|^2 r_{_T} dr_{_T} d\phi = \frac{1}{2\eta}|\mathcal{E}_0|^2\left[\frac{\pi w_0^2}{2}\right], \tag{23}$$

where η is the wave impedance of the homogeneous medium in which the beam propagates. Obviously, the power carried by the Gaussian beam is independent of z as it should be expected for any viable electromagnetic solution in a lossless medium.

2.3 Gaussian Beam Radius of Curvature

At this point let's comment on the radial phase shift factor observed in Eq. (20) of the fundamental Gaussian beam solution. In general, the scalar representation of a spherical

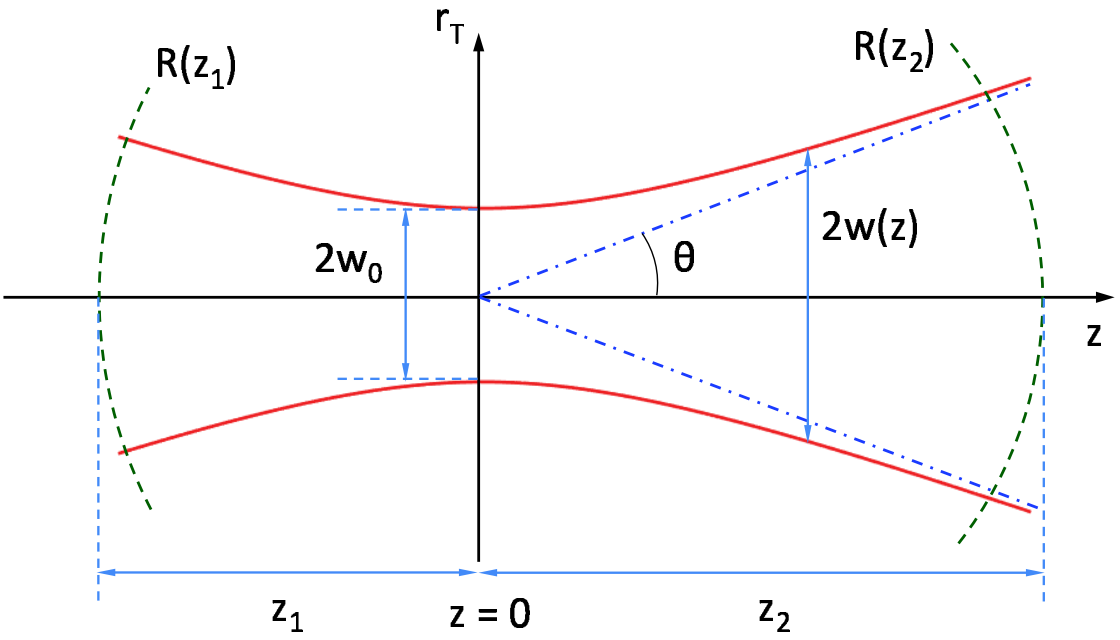

(a)

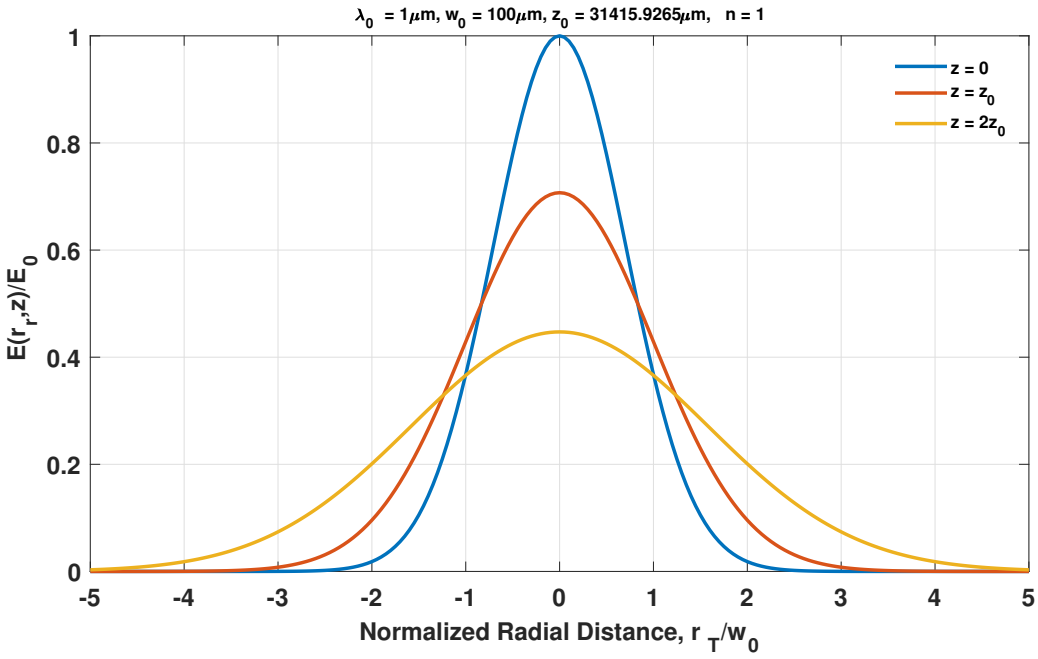

(b)

Figure 1: (a) A graphical representation of a Gaussian beam. The minimum beam waist, w_0, as well the beam waist at distance z, $w(z)$, and the radii of curvature, $R(z_1)$ and $R(z_2)$ at two, opposite to $z = 0$ distances z_1 and z_2 are shown. (b) Example profiles along the radial direction for various z's and for $\lambda_0 = 1\,\mu$m, $w_0 = 100\,\mu$m, and $n = 1$.

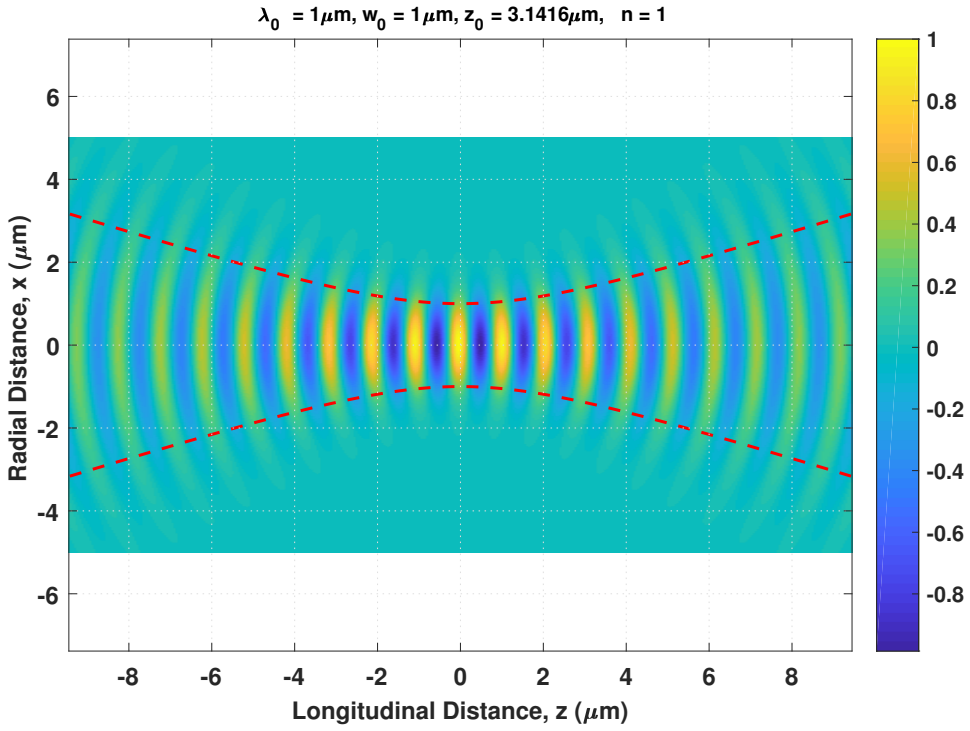

(a)

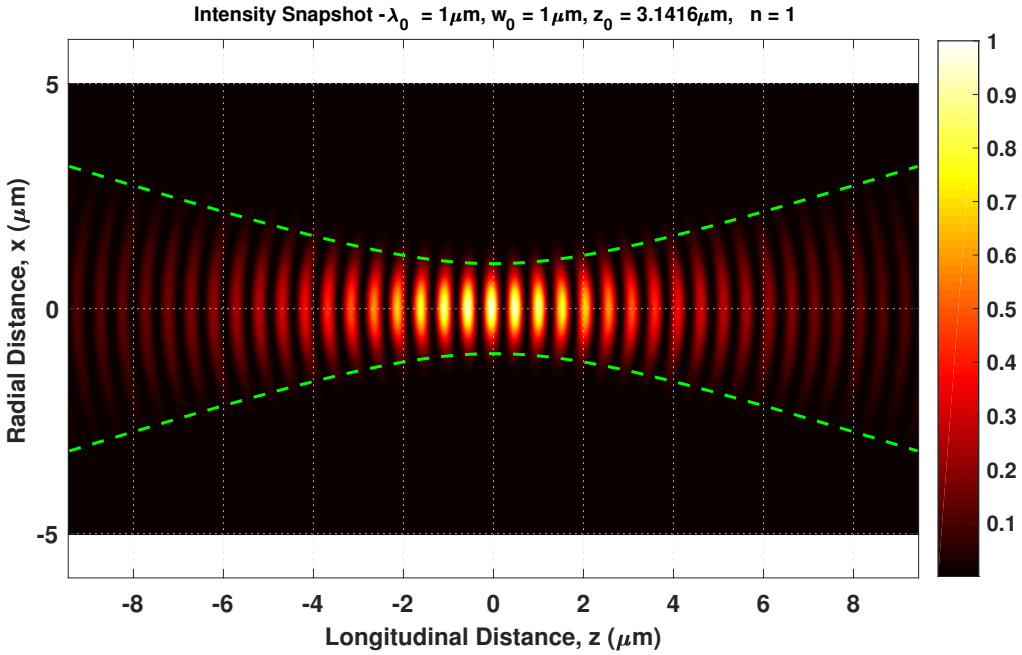

(b)

Figure 2: (a) A graphical representation of a Gaussian beam snapshot in time. The real electric field is shown in space for an instant of time. (b) The intensity $|E_{00}(r_{_T}, z)|^2$ snapshot. The example parameters are for $\lambda_0 = 1\,\mu$m, $w_0 = 1\,\mu$m, and $n = 1$.

wave (its electric field) is of the form

$$\begin{aligned} E_{sph} &= \frac{1}{r}\exp(-jkr), \quad \text{where} \\ r &= \sqrt{x^2+y^2+z^2} = \sqrt{r_{_T}^2+z^2} = z\sqrt{1+\frac{r_{_T}^2}{z^2}}. \end{aligned}$$

For $z \gg r_{_T}$ the following approximations can be made in the expression of the scalar plane wave:

$$\begin{aligned} r &\simeq z+\frac{1}{2}\frac{r_{_T}^2}{z} \simeq z+\frac{1}{2}\frac{r_{_T}^2}{r}, \quad \text{and} \\ E_{sph} &\simeq \frac{1}{r}\exp(-jkz)\exp\left(-j\frac{kr_{_T}^2}{2r}\right). \end{aligned} \tag{24}$$

Comparing the last term with the radial phase term of Eq. (20) the wavefront of the fundamental Gaussian beam of radius of curvature $R(z)$ evolves similarly to the spherical wave wavefront but with its center varying with z. Depending on the distance z from the beam's center the following approximations for $R(z)$ can be made (where z_c represents the position of the center of the spherical wavefront):

$$R(z) \simeq \begin{cases} +\infty, & \text{centered at} \quad z_c = \mp\infty, \quad \text{for} \quad |z| \ll z_0, \\ \mp 2z_0, & \text{centered at} \quad z_c = \mp z_0 \quad \text{for} \quad |z| = z_0, \\ z, & \text{centered at} \quad z_c = 0, \quad \text{for} \quad |z| \gg z_0. \end{cases} \tag{25}$$

2.4 Gaussian Beam Longitudinal Phase Shift - Gouy's Shift

The longitudinal phase shift of Eq. (20), $\Phi(z) = kz - \tan^{-1}(z/z_0)$, differs from the plane wave (or equivalently spherical wave) longitudinal phase shift, due to the term "$\tan^{-1}(z/z_0)$" which is known as Gouy's phase shift from the name of the M. Gouy who first discovered this type of phase shifts [3, 4]. There is a π phase shift for a fundamental Gaussian beam as it passes through its focal plane propagating from $z = -\infty$ to $z = +\infty$ relative to the phase shift that an ideal plane wave would have experienced. The Gouy phase shift is inherent to all spatially confined in the transverse (to the propagation direction) electromagnetic fields and can be derived from the transverse momenta of the monochromatic wave solution [5]. The phase of the Gaussian beam is related with the phase velocity of the beam (which can be greater than the velocity of light in free space!). Using the definition of Born and Wolf [6] the phase velocity of the fundamental Gaussian beam is given by

$$u_p = \frac{\omega}{d\Phi/dz} = \frac{\dfrac{c}{n}}{1-\dfrac{\lambda_0 z_0}{2\pi n}\dfrac{1}{z^2+z_0^2}}. \tag{26}$$

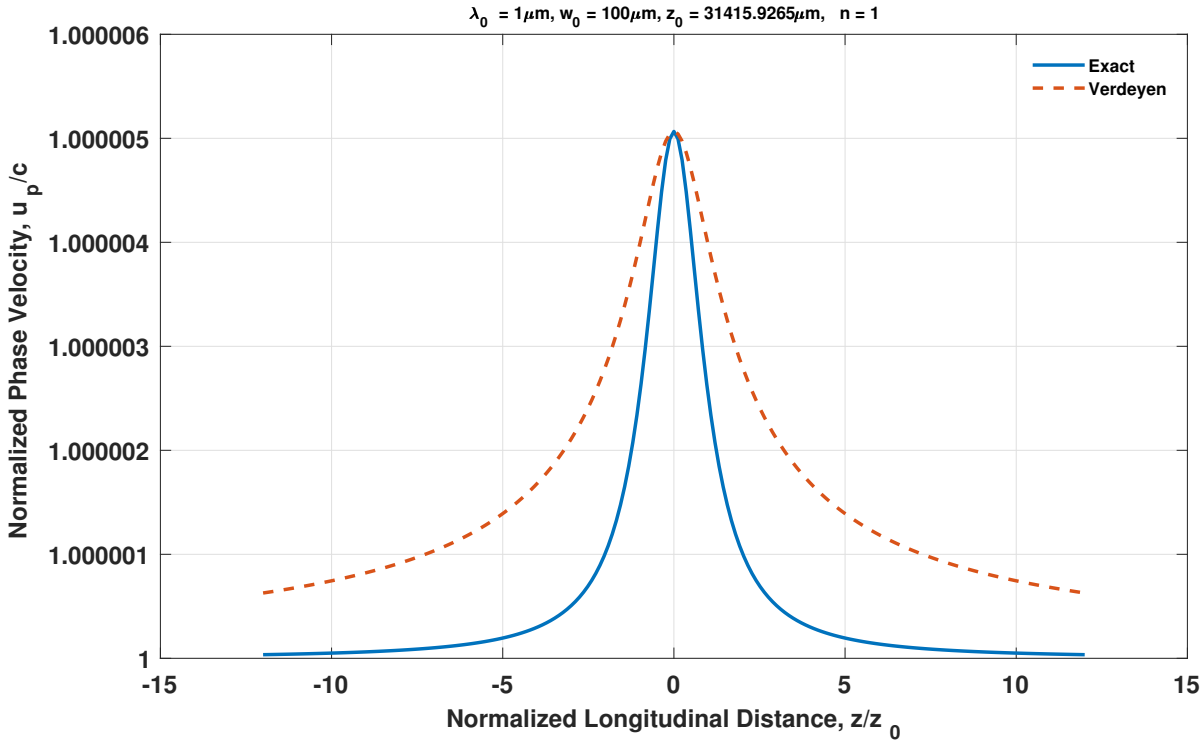

Figure 3: Phase velocity of the fundamental Gaussian beam along the longitudinal direction z for $\lambda_0 = 1\,\mu$m, $w_0 = 100\,\mu$m, and $n = 1$. Both the exact Eq. (26) and the approximate Eq. (27) solutions are shown.

In Verdeyen [2], an approximate expression of the phase velocity is given by

$$u_p = \frac{\omega}{\Phi/z} = \frac{\dfrac{c}{n}}{1 - \dfrac{\lambda_0}{2\pi n z}\,\tan^{-1}\left(\dfrac{z}{z_0}\right)}. \tag{27}$$

For example, the two phase velocities defined in Eqs. (26) and (27) are shown in Fig. 3. It can be observed that both phase velocities are greater (superluminal phase velocities) than the velocity of light in freespace near the focal plane of the Gaussian beam. However, this is not a surprise [7] since it can happen in other electromagnetic problems (an example is the phase velocity of the wave that travels parallel to a boundary where total internal reflection occurs for X-rays incident on crystals). This is not a violation of the fundamental law of physics (that the velocity of light in freespace is the greatest possible velocity) since any signal (i.e., information) will travel with a velocity which is always less than the velocity of light in freespace.

3 Higher-Order Hermite-Gaussian Beams

The fundamental Gaussian beam solution presented in Sec. 2 assumes no azimuthal dependence and therefore has cylindrical symmetry with respect to the axis of its propagation. However, in real laser resonators, more complicated beams can be generated. Assuming Cartesian geometry, higher-order Gaussian beam solutions can be found by solving the paraxial wave equation, Eq. (9). One family of the resulting solutions, named as TEM_{mp} Hermite-Gaussian beams is given by [1, 8]

$$\begin{aligned} E_{mp}(x,y,z) &= \mathcal{E}_{mp}^{HG} H_m\left(\frac{\sqrt{2}x}{w(z)}\right) H_p\left(\frac{\sqrt{2}y}{w(z)}\right) \frac{w_0}{w(z)} \exp\left[-\frac{x^2+y^2}{w^2(z)}\right] \\ &\quad \exp\left\{-j\left[kz-(1+m+p)\tan^{-1}\left(\frac{z}{z_0}\right)\right]\right\} \exp\left[-j\frac{k(x^2+y^2)}{2R(z)}\right], \quad (28) \end{aligned}$$

where,

$$\begin{aligned} w^2(z) &= w_0^2\left(1+\frac{z^2}{z_0^2}\right), \\ R(z) &= z\left(1+\frac{z_0^2}{z^2}\right), \\ H_m(u) &= (-1)^m e^{u^2}\frac{d^m}{du^m}\left(e^{-u^2}\right), \\ H_{m+1}(u) &= 2uH_m(u) - 2mH_{m-1}(u), \quad \text{with} \quad H_0(u)=1 \quad \text{and} \quad H_1(u)=u, \end{aligned}$$

where the functions H_m, H_p are Hermite polynomials of order m and p respectively ($m, p = 0, 1, 2, \cdots$). It is interesting to notice that the beam waist, $w(z)$, the radius of curvature $R(z)$, as well as the Rayleigh distance z_0, and the minimum beam waist w_0 are the same as in the fundamental Gaussian beam solution. Therefore, these higher-order beams experience the same divergence and power conservation property as the fundamental one. However, their Gouy phase shift, Φ_{Gouy}, is now given by

$$\Phi_{Gouy}(z) = (1+m+p)\tan^{-1}\left(\frac{z}{z_0}\right). \quad (29)$$

Similarly, their phase velocity is also affected and is given by

$$u_p = \frac{\omega}{d\Phi/dz} = \frac{\frac{c}{n}}{1-(1+m+p)\frac{\lambda_0 z_0}{2\pi n}\frac{1}{z^2+z_0^2}}. \quad (30)$$

The intensity patterns, $|E_{mp}(x,y,z=0)|^2$, of various Hermite-Gaussian beams are shown in their focal plane in Fig. 4.

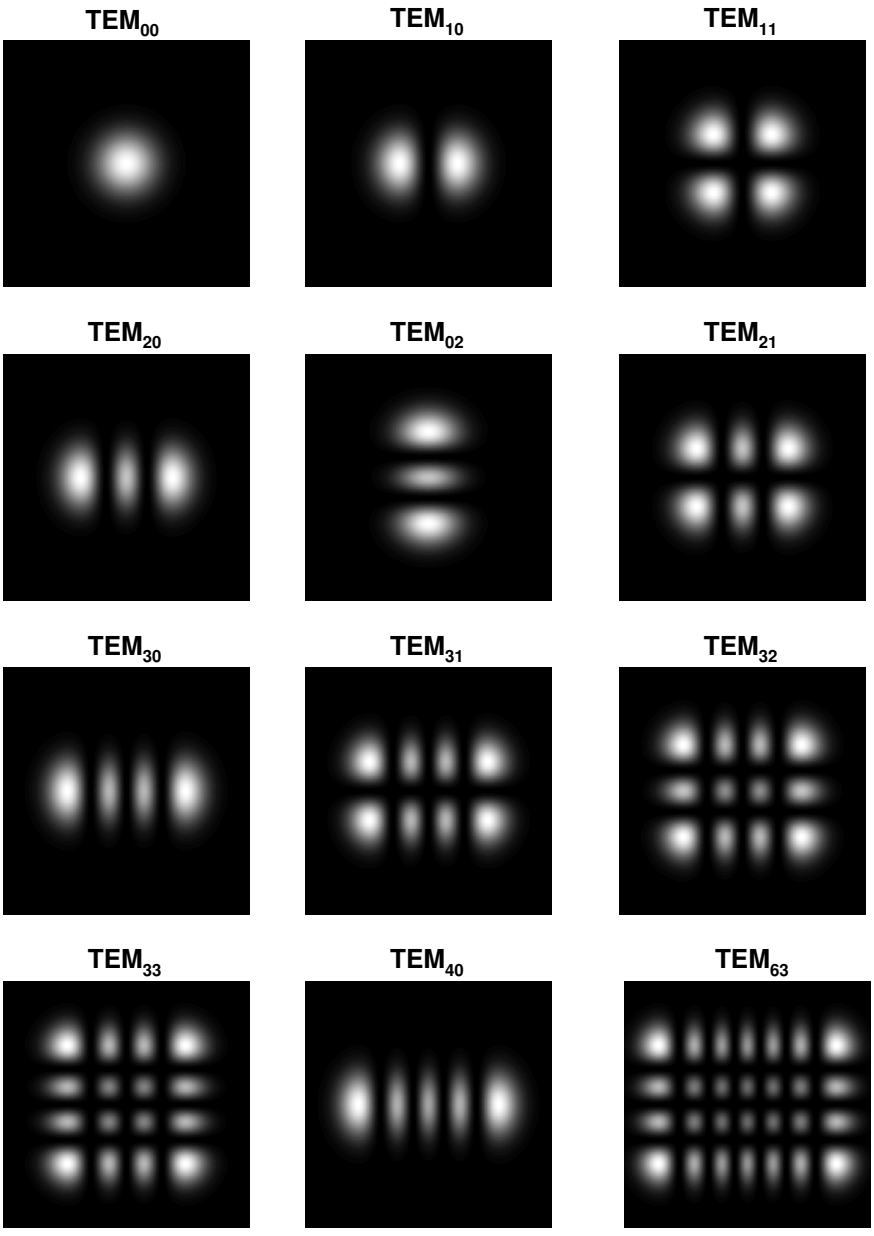

Figure 4: Intensity diagrams, $|E_{mp}(x, y, z = 0)|^2$, of some example Hermite-Gaussian beams for various values of m and p.

4 Higher-Order Laguerre-Gaussian Beams

An alternative and equivalent family of solutions of the paraxial wave equation in cylindrical coordinates with azimuthal dependence is known as TEM_{pm} Laguerre-Gaussian beams. The corresponding electric field components of these paraxial solutions is given below [1, 8]:

$$\begin{aligned} E_{pm}(r_{_T},\phi,z) &= \mathcal{E}_{pm}^{LG}\frac{w_0}{w(z)}\left(\frac{\sqrt{2}r_{_T}}{w(z)}\right)^{|m|} L_p^{|m|}\left(\frac{2r_{_T}^2}{w^2(z)}\right)\exp\left[-\frac{r_{_T}^2}{w^2(z)}\right] \\ &\quad \exp\left\{-j\left[kz-(1+|m|+2p)\tan^{-1}\left(\frac{z}{z_0}\right)\right]\right\}\exp(jm\phi)\exp\left[-j\frac{kr_{_T}^2}{2R(z)}\right], \quad (31) \end{aligned}$$

where,

$$\begin{aligned} w^2(z) &= w_0^2\left(1+\frac{z^2}{z_0^2}\right), \\ R(z) &= z\left(1+\frac{z_0^2}{z^2}\right), \\ L_p^m(u) &= \frac{e^u}{p!}u^{-m}\frac{d^p}{du^p}\left(e^{-u}u^{p+m}\right), \\ (k+1)L_{k+1}^p(u) &= (2k+1+p-u)L_k^p(u)-(k+p)L_{k-1}^p(u), \quad \text{with} \\ L_0^m(u) &= 1 \quad \text{and} \quad L_1^m(u)=-u+(m+1), \end{aligned}$$

and the functions $L_p^m(u)$ are the Laguerre polynomials, with the indices p and m being integers taking values $p = 0, 1, 2, \cdots$, and $m = 0, \pm1, \pm2, \cdots$. The integer m is related to the azimuthal dependence of the Laguerre-Gaussian beam solution through the term $\exp(jm\phi)$ that appears in Eq. (31). Linear combinations of Laguerre-Gaussian beams with $\pm m$ terms produce dependencies of $\cos(m\phi)$ and $\sin(m\phi)$. Laguerre-Gaussian beams with $m \neq 0$ have a property that Hermite-Gaussian modes do not possess. Specifically, Laguerre-Gaussian beams with $m \neq 0$ have a non-vanishing orbital angular momentum [8]. Actually, a Laguerre-Gaussian beam with $m \neq 0$ has an orbital angular momentum about the z axis that amounts to $m\hbar$ per photon [8]. Therefore, in principle, a Laguerre-Gaussian beam with $m \neq 0$ incident on an absorbing dielectric particle can cause the particle to rotate (this is a consequence of the conservation of the angular momentum). Laguerre-Gaussian beams are not usually produced by laser resonators, although it has been possible to generate such modes in lasers with very accurately aligned mirrors [8]. In general, any Laguerre-Gaussian beam can be expressed as a linear combination of Hermite-Gaussian beams and vice versa since both types of beams form complete sets [1,8]. The Gouy phase shift, Φ_{Gouy}, of Laguerre-Gaussian beams as well as their phase velocity are given by similar expressions as the ones used for the Hermite-Gaussian beams previously. The intensity patterns, $|E_{pm}(r_{_T},\phi,z=0)|^2$, of various Laguerre-Gaussian beams are shown in their focal plane in Fig. 5 for various values

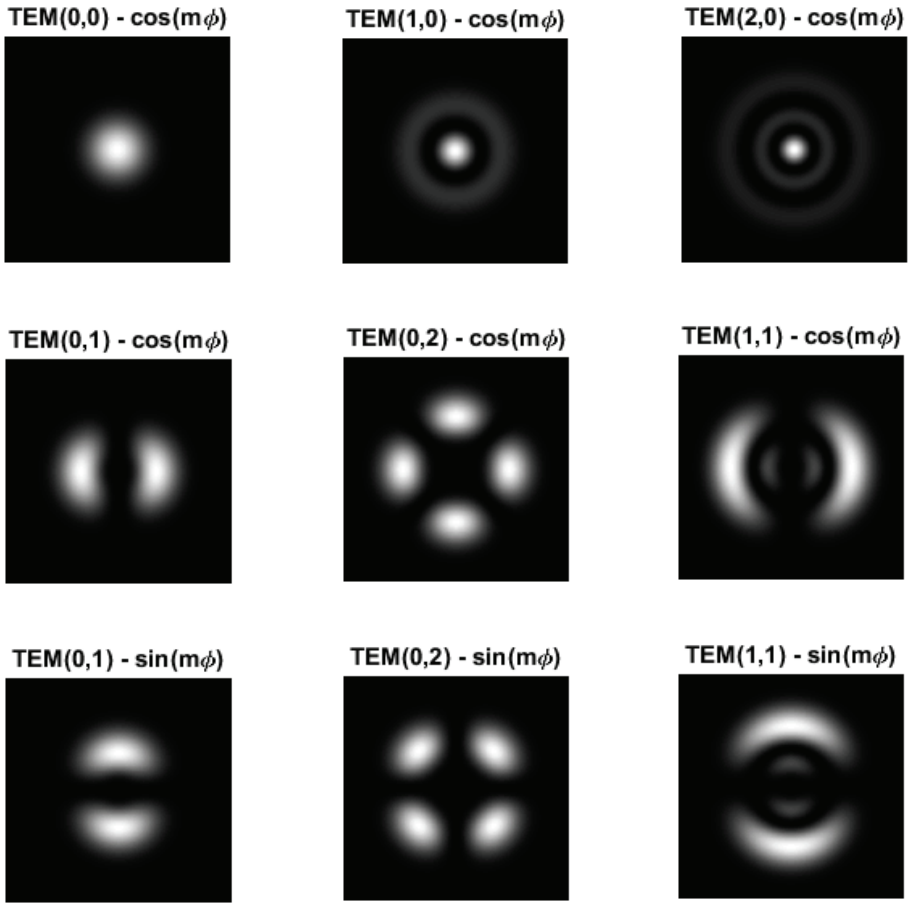

Figure 5: Intensity diagrams, $|E_{pm}(r_{_T}, \phi, z = 0)|^2$, of some example Laguerre-Gaussian beams for various values of m and p, and $\cos(m\phi)$ or $\sin(m\phi)$ dependence.

of m and p, and $\cos(m\phi)$ or $\sin(m\phi)$ dependence.

5 Validity of the Paraxial Approximation

An interesting question regarding the Gaussian beams (either Hermite-Gaussian of Laguerre-Gaussian) is the range of validity of these solutions which are based on the paraxial wave equation [Eq. (9)]. In Ref. [9] an integral method is used to determine the validity of paraxial beams based on the comparison between the vector Helmholtz equation and the paraxial

equation. In this reference a paraxiality parameter $\mathcal{P}$ is defined as

$$\begin{aligned} \mathcal{P} &= 1 - \frac{N+1}{k_0^2 n^2 w_0^2}, \qquad \text{where} \\ N &= m + p, \qquad \text{for Hermite-Gaussian beams,} \\ N &= 2p + |m|, \qquad \text{for Laguerre-Gaussian beams.} \end{aligned} \tag{32}$$

The closer to unity the paraxiality parameter $\mathcal{P}$ is, the better the performance of the paraxial approximation is. I.e., the solutions of the Helmholtz and the paraxial equations are very close, and the paraxial solutions give always meaningful and physical results.

6 The ABCD Law for Gaussian Beams

If q is the complex radius of curvature of a Gaussian beam [see Eq. (16)] then the ABCD law as it used in geometrical optics [2] can be applied to Gaussian beams. If for example, q_{in} is the input complex radius of curvature of a Gaussian beam entering an optical system (see Fig. 6a) that can be described by the paraxial ABCD matrix, then the emerging from the system output Gaussian beam has a complex radius of curvature q_{out} that is given by

$$q_{out} = \frac{Aq_{in} + B}{Cq_{in} + D}, \qquad \text{or} \tag{33}$$

$$\frac{1}{q_{out}} = \frac{C + D(1/q_{in})}{A + B(1/q_{in})}. \tag{34}$$

Therefore the ABCD matrices approach which is derived for paraxial rays (i.e., rays at small angles with respect to the propagation axis) in geometrical optics is also valid for paraxial beams as the Gaussian beams. This could be attributed to the geometrical optics rays being perpendicular to spherical wavefronts and to the spherical wavefronts (of varying origin) that were found for the Gaussian beam solutions. The transformation described in equations (33) and (34) can be easily proved in special cases such as in a Gaussian beam's propagation in a homogeneous medium or for a Gaussian beam passing through a thin lens, but in the general optical system case described by an ABCD matrix there is no formal proof, according to the author's knowledge. However, these equations are very useful in the analysis of Gaussian beams passing through optical systems assuming that the paraxial approximation is valid.

Example 6.1: As an example of applying the ABCD transformation rule for a Gaussian beam, the system shown in Fig. 6b is presented. A Gaussian beam is incident on a thin lens of focal length f from the left (assuming light propagation from left to right). The Gaussian beam is at its minimum spot size, w_{01}, at the left surface of the thin lens. The focal position L and the minimum spot size w_{03} of the emerging from the thin lens Gaussian beam are

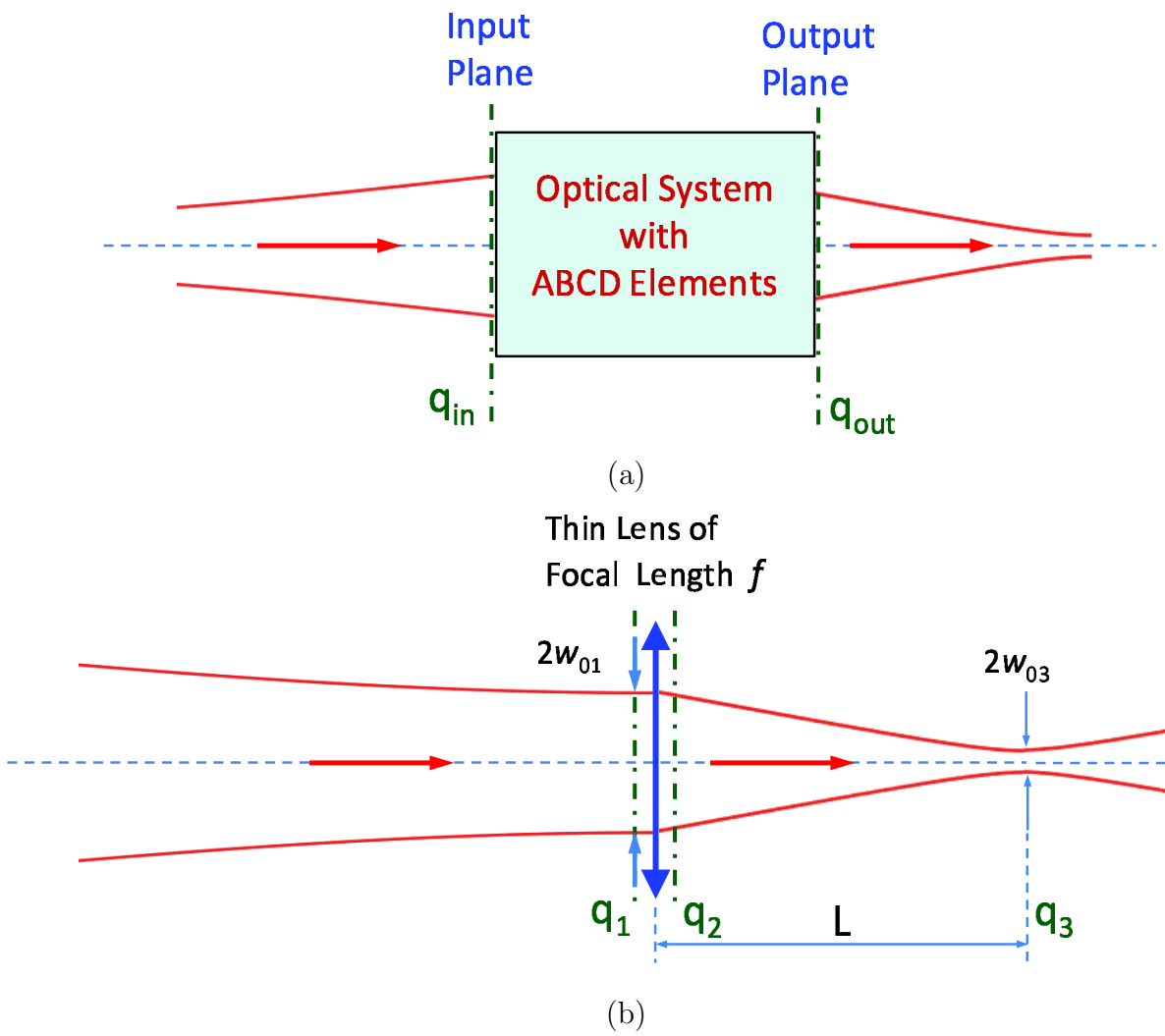

Figure 6: (a) A Gaussian beam with complex radius of curvature of q_{in} at the input plane of an optical system that can be described with the paraxial ABCD matrix. The Gaussian beam exiting the optical system has an output complex radius of curvature of q_{out}. (b) An example optical system comprised of a thin lens of focal length f. The Gaussian beam incident from the left is at its minimum waist, w_{01}, on the left surface of the thin lens.

sought.

Initially the ABCD elements of a thin lens are $A = 1$, $B = 0$, $C = -1/f$, and $D = 1$. Since the incident Gaussian beam is focused on the left side of the thin lens $1/q_1 = -j\lambda_0/\pi n w_{01}^2$ (since $R_1 = R(z = 0) = \infty$). Applying Eq. (34) the q_2 on the right surface of the thin lens is given by

$$\frac{1}{q_2} = \frac{C + D(1/q_1)}{A + B(1/q_1)} = -\frac{1}{f} + \frac{1}{q_1} = -\frac{1}{f} - j\frac{\lambda_0}{\pi n w_{01}^2} = a + jb, \tag{35}$$

where $a = -1/f$ and $b = -\lambda_0/\pi n w_{01}^2 = -1/z_{01}$, with z_{01} the Rayleigh distance of the

Gaussian beam incident from the left. From the right surface of the thin lens the emerging Gaussian beam propagates in homogeneous space for a distance L (still unknown) where it is expected to focus. For a homogeneous space the corresponding ABCD matrix elements are $A = 1$, $B = L$, $C = 0$, and $D = 1$. Therefore, applying once more Eq. (34) it can be shown that

$$\begin{aligned}\frac{1}{q_3} &= \frac{C + D(1/q_2)}{A + B(1/q_2)} = \frac{1/q_2}{1 + L/q_2} = \frac{a + jb}{(1 + aL) + jbL} = \\ &= \frac{a(1 + aL) + Lb^2}{(1 + aL)^2 + L^2b^2} - j\frac{-b}{(1 + aL)^2 + L^2b^2} = \\ &= \frac{1}{R_3} - j\frac{\lambda_0}{\pi n w_{03}^2}. \end{aligned} \tag{36}$$

However at $z = L$ the emerging Gaussian beam should be focused. Therefore $R_3 = \infty$ and $1/R_3 = 0$. Then, the real part of the last equation is zero and L can be determined as,

$$\begin{aligned} a(1 + aL) + Lb^2 &= 0 \quad \Longrightarrow L = \frac{-a}{a^2 + b^2} \quad \Longrightarrow \\ L &= \frac{f}{1 + \left(\dfrac{f}{z_{01}}\right)^2}. \end{aligned} \tag{37}$$

Since L is found, from the imaginary part of Eq. (36) the w_{03} can also be determined, after some algebra, and is given by

$$w_{03} = w_{01}\,\frac{\dfrac{f}{z_{01}}}{\left[1 + \left(\dfrac{f}{z_{01}}\right)^2\right]^{1/2}}. \tag{38}$$

The complex curvature $1/q_3$ could also be determined in one step from $1/q_1$ if the properties of the ABCD matrices are used. In the latter case the ABCD matrix elements that should be used in Eq. (34) result from the combination of the thin lens and homogeneous propagation matrices and are $A = 1 - L/f$, $B = L$, $C = -1/f$, and $D = 1$. At this point it is interesting to assume some numerical values. For a He-Ne laser produced Gaussian beam the freespace wavelength for the red light is $\lambda_0 = 0.6328\,\mu$m. Assume that the minimum beam waist of the incident from the left Gaussian beam is $w_{01} = 1\,$cm (i.e. it is a well collimated beam incident on the thin lens). The thin lens has a focal length of $f = 10\,$cm. Furthermore, let's assume that the power of the laser is $P = 10\,$mW (typical value for a He-Ne laser). Then the Rayleigh distance of the incident Gaussian beam is $z_{01} = \pi n w_{01}^2/\lambda_0 = 496.459\,m \simeq 0.5\,$km! (it is also assumed that $n = 1$, i.e., the beam propagates in air). The focal distance L is

easily found from Eq. (37) and is equal to $L \simeq 10\,cm = f$. Therefore, the result is the one expected for a thin lens under the paraxial geometrical optics approximation. This happens due to the well collimated and relatively wide indicent Gaussian beam. The minimum beam waist of the emerging from the thin lens Gaussian beam is given by Eq. (38) and is $w_{03} = 2.0143\,\mu$m! Even for such a small focused beam waist, the Gaussian beam solution is valid and reliable since the paraxiality parameter $\mathcal{P} = 1 - 1/k_0^2 n w_{03}^2 \simeq 0.9975$, i.e., it is still very close to unity [9]. Finally, the power density at the focal plane is $I_3 \simeq P/(\pi w_{03}^2) = 7.8454 \times 10^8\,W/m^2 = 78.454\,KW/cm^2$ which is significant despite the very moderate power of the laser. This shows how with an optical system (in this case a simple thin lens) the laser beam can be focused in a very small area for achieving nonlinear effects such as cutting a target.

References

[1] A. E. Siegman, *Lasers*. California: University Science Books, 1986.

[2] J. T. Verdeyen, *Laser Electronics*. New Jersey: Prentice Hall, 3rd ed., 1995.

[3] M. Gouy, "Sur une propriètè nouvelle des ondes lumineuses," *C. R. Acad. Sci. Paris*, vol. 110, pp. 1251–1253, 1890.

[4] M. Gouy, "Sur la propagation anomale des ondes," *Ann. Chim. Phys. 6*, vol. XXIV, pp. 145–213, 1891.

[5] S. Feng and H. G. Winful, "Physical origin of the Gouy phase shift," *Opt. Lett.*, vol. 26, pp. 485–487, Apr. 2001.

[6] M. Born and E. Wolf, *Principles of Optics*, ch. 1. New York: Cambridge University Press, 7th ed., 1999.

[7] J. Weber, "Phase, group, and signal velocity," *Amer. J. Phys.*, vol. 22, pp. 618–620, 1954.

[8] P. W. Milonni and J. H. Eberly, *Laser Physics*. Hoboken, New Jersey: John Wiley & Sons, Inc., 2010.

[9] P. Vaveliuk, B. Ruiz, and A. Lencina, "Limits of the paraxial approximation in laser beams," *Opt. Lett.*, vol. 32, pp. 927–929, Apr. 2007.